Aquaculture 612 (2026) 743187

Contents lists available at ScienceDirect

Aquaculture

journal homepage: www.elsevier.com/locate/aquaculture

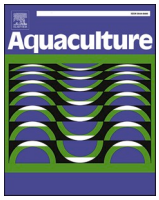

Consequences of meiosis in first-generation hybrids derived from *Megalobrama amblycephala* (♀) and *Culter alburnus* (♂)

Yingying Yang [a,1], Lang Qin [a,1], Hongxuan Liang [a,1], Jiawang Huang [a], Ming Wen [a], Yuxiang Wang [a], Le Shen [a], Jinhui Huang [a], Xu Huang [a,b], Fangzhou Hu [a,b], Shi Wang [a], Chang Wu [a,b,c,d,*], Shaojun Liu [a,b,d,*]

[a] *Engineering Research Center of Polyploid Fish Reproduction and Breeding of the State Education Ministry, College of Life Sciences, Hunan Normal University, Changsha, China*
[b] *Yuelushan Laboratory, Changsha, China*
[c] *Hunan Province Fish Fry Breeding Technology Co., Ltd., Wugang, China*
[d] *Institute of Interdisciplinary Studies, Hunan Normal University, Changsha, China*

ARTICLE INFO

Keywords:
Hybridization
Gynogenesis
Allodiploid gynogenetic fish
Microsatellite
Transcriptome analysis

ABSTRACT

Gynogenesis and distant hybridization are two techniques prevalently used for genetic breeding of fish. In artificially induced gynogenetic progeny, nuclear genetic material is derived from the duplication of the egg's chromosomes, making these progeny ideal models for exploring the meiotic characteristics of hybrid offspring. The hybrid BTF_1 was produced by crossing *Megalobrama amblycephala* (blunt snout bream, BSB, 2n = 48, ♀) with *Culter alburnus* (topmouth culter, TC, 2n = 48, ♂). The gynogenetic BTF_1 ($GBTF_1$) was induced using UV-irradiated sperm from common carp (*Cyprinus carpio*, 2n = 100, ♂), followed by chromosome doubling by cold shock. This process yielded two types of offspring with notable differences in appearance, designated $GBTF_1$-B and $GBTF_1$-M. The DNA content and chromosome number were analyzed, revealing that both $GBTF_1$-B and $GBTF_1$-M were diploids, each possessing 48 chromosomes. Meanwhile, the microsatellite amplification results showed that 39.92 % and 39.36 % of bands in $GBTF_1$-B and $GBTF_1$-M were consistent with both BSB and TC, 36.75 % and 23.77 % bands consistent with only BSB, 14.19 % and 20.97 % bands consistent with only TC, and 9.14 % and 15.90 % bands from mutation, respectively. The results indicated that BTF_1 produced heterozygous gametes with unevenly distributed genetic material of BSB and TC during meiosis. In addition, expression analysis of homologous genes showed that 15.3–20.33 % and 6.96–8.43 % differentially expressed genes (DEGs) in $GBTF_1$-B were biased to BSB and TC. In contrast, 10.40–14.39 % and 10.60–14.19 % DEGs in $GBTF_1$-M were biased to BSB and TC, respectively. The results suggested that the expression model of DEGs in $GBTF_1$-B was more biased towards BSB, whereas $GBTF_1$-M exhibited an intermediate expression pattern between BSB and TC. These findings demonstrated the heterogeneity of gametes produced by the first-generation hybrid fish. This research provides a genomic reference for understanding the outcomes of meiosis in hybrid fish and offers valuable insights into fish reproduction and breeding.

1. Introduction

Gynogenesis and hybridization are traditional but effective techniques for fish genetic breeding (Liu et al., 2025). Gynogenesis can be classified into two types, natural gynogenesis and artificial gynogenesis (Wu et al., 2019; Xu et al., 2015). Artificial gynogenesis generally involves a two-step process: activation of the egg by radiation-inactivated sperm, followed by chromosome doubling (Li et al., 2018; Mao et al.,

Abbreviation: BSB, blunt snout bream; TC, topmouth culter; BTF_1, first filial generation of BSB (♀) × TC (♂); $GBTF_1$, gynogenetic BTF_1; $GBTF_1$-B, BSB-like-type in $GBTF_1$; $GBTF_1$-M, intermediate-type in $GBTF_1$; $GBTF_1$-T, TC-like-type in $GBTF_1$; FL, full length; BL, body length; BH, body height; HH, head height; HL, head length; ELD-BSB, expression level dominance-BSB; ELD-TC, expression level dominance-TC; DEGs, differentially expressed genes.

* Corresponding authors at: Engineering Research Center of Polyploid Fish Reproduction and Breeding of the State Education Ministry, College of Life Sciences, Hunan Normal University, Changsha 410081, China.
E-mail addresses: wuchang@hunnu.edu.cn (C. Wu), lsj@hunnu.edu.cn (S. Liu).
[1] These authors contributed equally to this work.

https://doi.org/10.1016/j.aquaculture.2025.743187
Received 9 July 2025; Received in revised form 1 September 2025; Accepted 11 September 2025
Available online 12 September 2025

2019; Sun et al., 2007). This two-step process is widely applied in fish genetics and breeding (Ban et al., 2013; Chen et al., 2017; Miao et al., 2014). Natural gynogenesis is widely found in many species in nature (Brykov et al., 2002; Xiao et al., 2011; Zhou et al., 2000), and distant hybridization is also a common way to produce natural gynogenetic offspring (Fan et al., 2024; Qin et al., 2015; Wu et al., 2003). Distant hybrid progenies normally have a hybrid genome with maternal and paternal genetic material from two different species(Liu et al., 2022; Yang et al., 2025). However, previous studies have shown that the progeny resulting from both natural and artificial gynogenesis contain mainly genetic material from the female parent, with only a small insertion of genetic material from the male parent (Chen et al., 2020; Liu et al., 2025; Portemer et al., 2015). Due to the occurrence of genomic shock, the genomes of first-generation hybrids are often unstable, resulting in phenotypic segregation in the second generation.

Microsatellites, also called simple sequence repeats (SSR), are tandem repeat sequences consisting of a few nucleotides (typically 1 to 6) through multiple repeat units (Tóth et al., 2000). Due to their high polymorphism, stability, reproducibility, and ability to reflect the genetic structure and genetic diversity of species, microsatellites are considered ideal genetic molecular markers (Foster et al., 2020; Marwal and Gaur, 2020). In addition, owing to the simplicity of microsatellite amplification, microsatellites have been widely applied in studies of genetic variation and divergence in fish gynogenesis and distant hybridization (Anil et al., 2016; Wooten et al., 2018). RNA-sequencing enables the comprehensive and rapid acquisition of sequence and expression information for nearly all transcripts within a specific cell or tissue under defined conditions. Investigating gene expression patterns in gynogenetic and hybrid fish is essential for understanding gene inheritance and variation in these two processes (Kukurba and Montgomery, 2015; Ren et al., 2017; Zhao et al., 2024).

Megalobrama amblycephala (blunt snout bream, BSB, 2n = 48) and *Culter alburnus* (topmouth culter, TC, 2n = 48) are two economically important freshwater fish species in China, demonstrating good growth rates and meat quality, respectively (Zheng et al., 2019). The advantages of BSB and TC can be combined through distant hybridization to produce hybrid progeny with fast growth and high meat quality. Previously, bisexual fertile allodiploids (BTF_1) were obtained by crossing BSB (♀) with TC (♂), both of which can undergo meiosis normally and produce haploid gametes (Xiao et al., 2014; Zhou et al., 2015). To further investigate the genetic composition of these haploid gametes, gynogenetic BTF_1 ($GBTF_1$) were obtained by using sperm from common carp (*Cyprinus carpio*, 2n = 100, ♂) to induce gynogenesis in eggs of BTF_1. Following distant hybridization and artificial gynogenesis, microsatellite and transcriptome analysis were conducted on $GBTF_1$ to investigate its genetic composition and expression pattern, elucidating the genetic variation during the meiosis progress of hybrids.

2. Materials and methods

2.1. Ethics statement

The guidelines established by the Administration of Affairs Concerning Animal Experimentation state that approval from the Science and Technology Bureau of China and the Department of Wildlife Administration is not necessary when the fish in question are neither rare nor near extinction (first- or second-class state protection level). Therefore, approval was not required for the experiments described in this manuscript. The fish were strongly anesthetized with 100 mg/L MS-222 (Sigma–Aldrich, St. Louis, MO, USA) prior to dissection. All personnel involved in fish care and experimentation were certified through a professional training course for laboratory animal practitioners held by the Institute of Experimental Animals, Hunan Province, China.

2.2. Animals and gynogenesis

The parent fish were cultivated in the Engineering Research Center of Polyploid Fish Reproduction and Breeding of the State Education Ministry, Hunan Normal University. During the reproductive season (May to July) in 2018, a total of 40 sexually mature female BTF_1 and 20 male common carp were randomly selected to form 40 batches for this experiment, including 28 batches for artificially induced gynogenesis and 6 batches for each control group: BTF_1 (♀) × UV-treated common carp (♂) without cold shock treatment, and BTF_1 (♀) × common carp (♂). Appropriate amounts of oxytocin were injected (Liu et al., 2022), and the gametes were collected.

The collected common carp milt was diluted with Hank's solution at a ratio of 1:4. Subsequently, 3 mL of diluted milt was spread evenly in a 25 mL culture dish and irradiated under ultraviolet light until the percentage of motile sperm was reduced to about 50 % (Qin et al., 2018). Two ultraviolet lamps with a rated power of 15 watts each was used, and the distance between the ultraviolet lamps and the samples was 20 to 30 cm. Mature eggs from BTF_1 were treated with the above sperm to activate and initiate embryonic development. After 2–5 min of fertilization, the fertilized eggs were treated at 4–6 °C for 12–18 min to inhibit the extrusion of the second polar body from the fertilized eggs to induce the doubling of the nuclear genetic material. Thereafter, the fertilization rate (number of survival embryos at the gastrula stage/total number of eggs) and the hatching rate (number of hatched fry/total number of fertilized eggs) were calculated for each group of 2000 embryos and analyzed for comparison.

2.3. Morphological traits

With BSB and TC as controls, 15 $GBTF_1$-B and 15 $GBTF_1$-M individuals were randomly selected to analyze the countable and measurable traits of the $GBTF_1$. Countable traits included the number of lateral line scales, upper and lower lateral line scales, and the numbers of rays in the abdominal, dorsal and anal fins. The measurable traits included full length (FL), body length (BL), body height (BH), head height (HH), and head length (HL). To further minimize the error, the ratios between the measurable traits were compared, and SPSS software was used to calculate the *P* value for statistical analysis and error analysis.

2.4. Determination of ploidy level

To confirm that these $GBTF_1$ were not haploids or triploids formed by incomplete cold shock or fusion with sperm with insufficient ultraviolet exposure, the ploidy level was determined by flow cytometry (Partec). After 15 months of culture in specialized pools, blood was collected from the caudal vein of 15 randomly selected $GBTF_1$-B and 15 $GBTF_1$-M individuals. Erythrocyte DNA content from BSB, and TC specimens were served as controls. The blood samples were treated successively with sodium heparin and DAPI DNA staining solution (Partec), as outlined by previous studies (Liu et al., 2001; Wu et al., 2020). The χ^2 tests with Yates' correction were performed to assess deviations from expected values in these samples. In addition, the caudal vein blood of each $GBTF_1$ sample was cultured in vitro by the method described by (Luo et al., 2011) to prepare the chromosome spreads at metaphase. The chromosome numbers were counted and recorded under a microscope. Then, each three individuals of $GBTF_1$-B and $GBTF_1$-M were randomly selected to be performed on further microsatellite detection and expression analysis of homologous genes.

2.5. Microsatellite detection

Based on the flow cytometry, chromosome analysis, and morphological traits, the $GBTF_1$ specimens were preliminarily categorized into two types, namely the BSB-like-type in $GBTF_1$ ($GBTF_1$-B) and

Table 1
The fertilization rate and hatching rate of the cold-shock-treated BTF_1 (♀) × UV-treated common carp (♂), non-cold-shock-treated BTF_1 (♀) × UV-treated common carp (♂) and BTF_1 (♀) × common carp (♂) groups.

Ratio	Gynogenesis	Control groups	
	$GBTF_1$	BTF_1 (♀) × UV-treated common carp (♂) without cold shock	BTF_1 (♀) × common carp (♂)
Fertilization rate (%)	91.50 ± 0.52	90.05 ± 0.78	91.50 ± 0.53
Hatching rate (%)	6.5 ± 0.29	19.69 ± 0.94	0

intermediate-type in $GBTF_1$ ($GBTF_1$-M). The microsatellite primers (**Supplemental Table 1**) mentioned in (Su et al., 2019; Tang et al., 2017) (in Chinese) were selected to amplify the microsatellite markers in 3 BSB, 3 TC, 3 $GBTF_1$-B, and 3 $GBTF_1$-M to investigate the genetic composition of $GBTF_1$. The genomes were extracted from the liver tissue of each fish sample using the DNA kit (Takara, Beijing, China) following the manufacturer's instructions. Subsequently, PCR products were separated by 8 % polyacrylamide electrophoresis and then visualized by silver nitrate (Sanguinetti and Simpson, 1994). The gel was washed with pure water and photographed. Finally, the bands were categorized and counted based on their correspondence to the original biparental profiles.

2.6. Expression analysis of homologous genes

In order to investigate the divergence in the expression level of $GBTF_1$ and its original parents, next-generation transcriptome sequencing was performed on liver tissues of BSB, TC, $GBTF_1$-B, and $GBTF_1$-M. 3 individuals were randomly selected from each of the four types of fish for liver tissue isolation and extraction of complete RNA by the Trizol method (Liu et al., 2018). The integrity of the RNA was examined by Agilent 2100, and samples that met the quality standards were sequenced. The raw data of the above 12 samples were combined and assembled into transcripts by a de novo method. The mixed transcripts of these 12 samples were then clustered using CD-HIT software

Table 2
The countable traits of BSB, TC, $GBTF_1$-B and $GBTF_1$-M.

Fish type	Lateral line scales	Upper lateral line scales	Lower lateral line scales	Dorsal fin rays	Abdominal fin rays	Anal fin rays
BSB[a]	49–52	9–10	9-11	III + 8–9	8–10	III + 25–27
TC[a]	80-92	16-19	6-7	III + 7	9	III + 20–23
$GFBF_1$-B	52–56	9–10	9–10	III + 8–9	8–9	III + 25–26
$GFBF_1$-M	60–62	11–12	9–11	III + 8	9–10	III + 22–25

III. The number of fin spines.
[a] Data from (Xiao, 2013).

Table 3
The measurable traits of BSB, TC, $GBTF_1$-B and $GBTF_1$-M.

Fish type	FL/BL	BL/BH	BL/HH	HL/HH
BSB[a]	1.18 ± 0.02	2.36 ± 0.04	2.08 ± 0.05	1.19 ± 0.06
TC[a]	1.18 ± 0.03	3.97 ± 0.23	2.27 ± 0.01	2.18 ± 0.27
$GFBF_1$-B	1.18 ± 0.04	2.37 ± 0.08	2.10 ± 0.06	1.20 ± 0.15
$GFBF_1$-M	1.20 ± 0.03	3.30 ± 0.15	2.24 ± 0.16	1.52 ± 0.12

[a] Data from (Xiao, 2013).

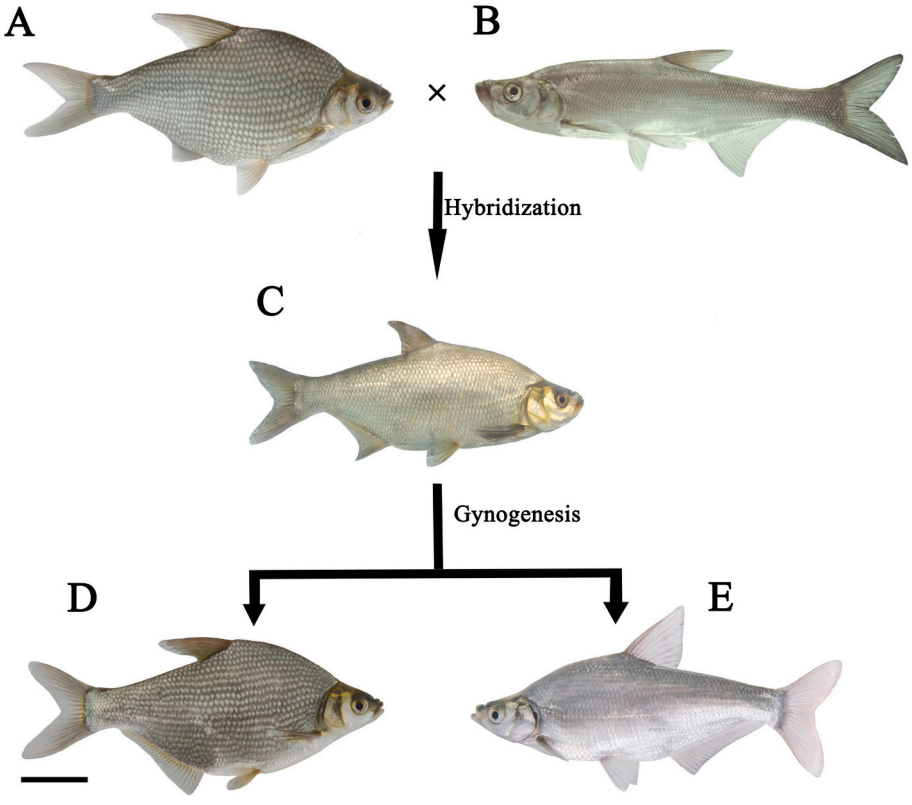

Fig. 1. The establishment procedure and profile of $GBTF_1$. (A) BSB: blunt snout bream. (B) TC: topmouth culter. (C) BTF_1: first filial generation of BSB (♀) × TC (♂). (D) $GBTF_1$-B: BSB-like-type in $GBTF_1$. (E) $GBTF_1$-M: intermediate-type in $GBTF_1$. Bar = 3 cm.

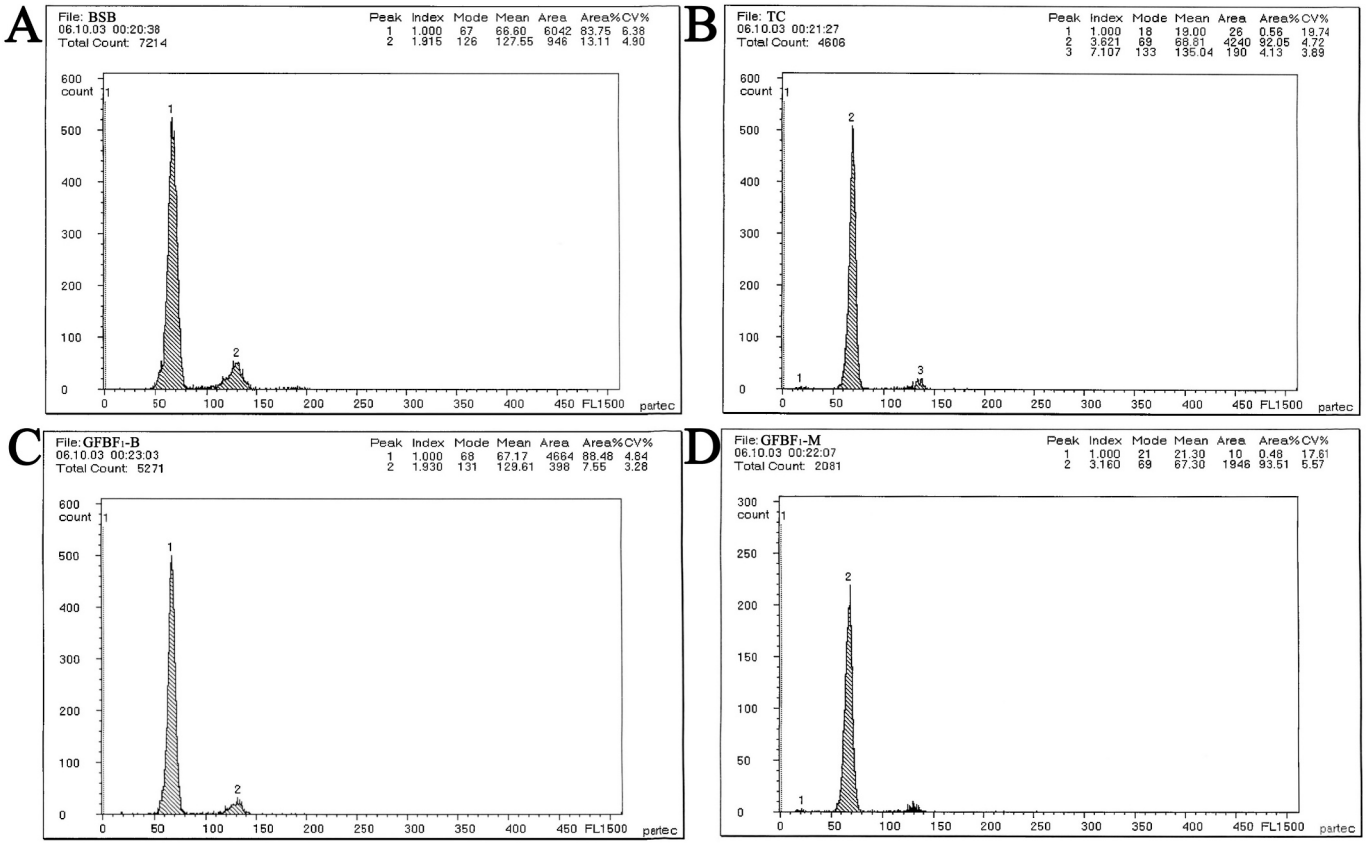

Fig. 2. Cytometric histogram of DNA fluorescence for BSB, TC, $GBTF_1$-B and $GBTF_1$-M. (A) The mean DNA content of BSB (peak 1: 66.60). (B) The mean DNA content of TC (peak 2: 68.81). (C) The mean DNA content of $GBTF_1$-B (peak 1: 67.17). (D) The mean DNA content of $GBTF_1$-M (peak 2: 67.30).

(threshold = 95 %) to remove the redundant sequences. The most representative transcripts were selected and used as reference sequences. Thereafter, the clean reads of each sample were mapped to the reference transcripts, and the respective RPKM values were calculated. Genes expressed simultaneously in BSB, TC, $GBTF_1$-B, and $GBTF_1$-M were identified as homologous gene sets. Differentially expressed genes (DEGs) in $GBTF_1$-B and $GBTF_1$-M were identified by comparing their expression levels to those of BSB or TC, respectively. Homologous genes showing significant expression differences were screened using DEseq2, with thresholds set at FDR < 0.05 and $|\text{Log2 (Fold change)}| > 1$. By referring to (Rapp et al., 2009), we divided DEGs into 5 expression modes and 10 categories including up-regulation (I, II), ELD-BSB (III, IV), ELD-TC (V, VI), down-regulation (IX, X), and additive expression pattern (VII, VII). According to the method mentioned in (Zhou et al., 2015), DEGs whose expression level in $GBTF_1$ was not significant different from mid-parent value, the average expression value of DEGs in BSB and TC, were demonstrated as additive expression pattern ($P < 0.05$ to indicate the significant difference; Fisher's exact tests). Furthermore, ELD-BSB (expression level dominance-BSB) indicated that expression level of a DEG in $GBTF_1$ was similar to BSB and significantly different from TC, and ELD-TC (expression level dominance-TC) indicated that expression level of a DEG in $GBTF_1$ was similar to TC and significantly different from BSB ($P < 0.05$; Fisher's exact tests). Up-regulation and down-regulation expression modes indicated that the expression level of a DEG in $GBTF_1$ was significantly different from that in both BSB and TC, and was higher or lower than its expression levels in BSB and TC ($P < 0.05$; Fisher's exact tests). Finally, the number of DEGs expressed under each mode and category was counted in $GBTF_1$-B and $GBTF_1$-M. Ten representative genes from the above five expression modes were subjected to qRT-PCR to verify the presence of each expression pattern in $GBTF_1$-B and $GBTF_1$-M.

3. Results

3.1. Induction gynogenesis of BTF_1

In this experiment, one experimental group and two control groups were set up. In the experimental group, inactivated sperm from common carp successfully activated the eggs of BTF_1, and the nuclear genetic materials of the activated eggs were doubled by cold shock treatment. A total of approximately 42,000 viable $GBTF_1$ fries were obtained, with an emergence rate of 3.58 %–5.36 %. In contrast, in the control group where BTF_1 eggs were activated with inactivated sperm but without chromosome doubling, only malformed fries were obtained. These showed a haploid syndrome and died after a few days (Zhou et al., 2022). In the other control group, BTF_1 was directly crossed with the common carp, and the embryos did not survive past the gastrula stage. The specific fertilization rate and hatching rate are shown in Table 1.

3.2. Morphological traits

The first generation of gynogenic progeny of BTF_1, named $GBTF_1$, was successfully obtained by the induction of gynogenesis of BTF_1. The preparation process and the appearance of $GBTF_1$ are shown in Fig. 1; its countable and measurable traits are shown in Table 2 and Table 3. The $GBTF_1$ individuals were divided into two body types according to their morphology. One had a similar appearance to BSB and was named bream-type gynogenetic BTF_1 ($GBTF_1$-B, Fig. 1 D). The other developed an appearance similar to the hybrid progeny of BSB and TC, which was named intermediate-type gynogenetic BTF_1 ($GBTF_1$-M, Fig. 1 E). The results indicated that the number of lateral line scales, upper and lower lateral line scales, and the number of rays in abdominal, dorsal, and anal fins of $GBTF_1$-B were biased towards BSB ($P > 0.05$). Additionally, the

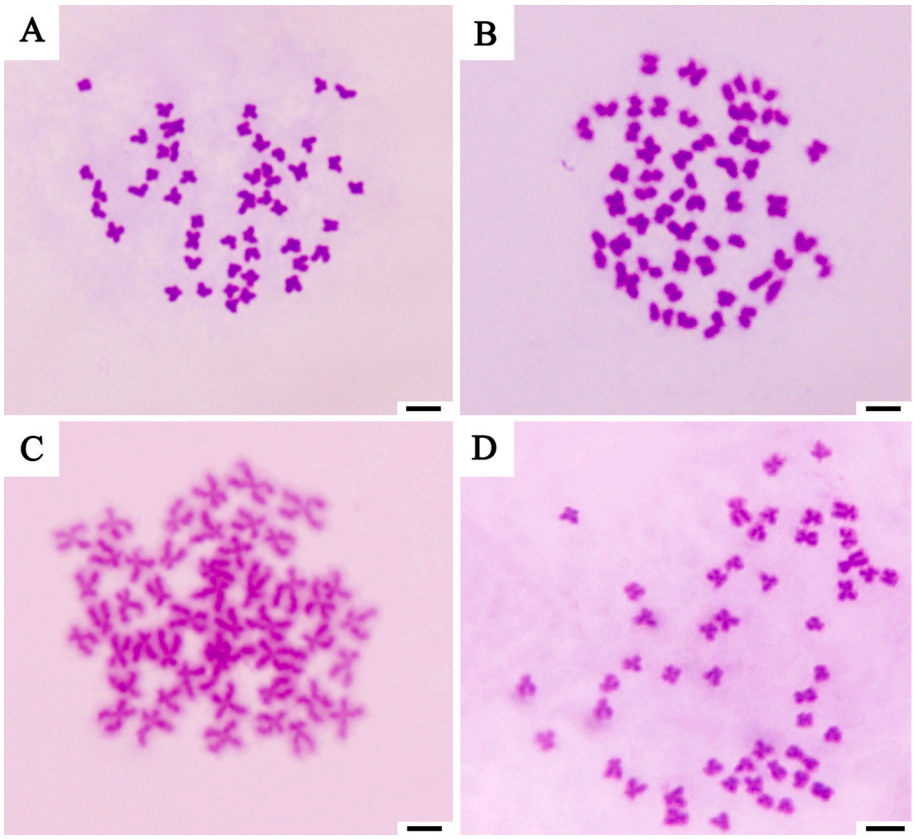

Fig. 3. The chromosome spreads at metaphase in BSB, TC, $GBTF_1$-B and $GBTF_1$-M. (A) The chromosome spreads of BSB. (B) The chromosome spreads of TC. (C) The chromosome spreads of $GBTF_1$-B. (D) The chromosome spreads of $GBTF_1$-M. Bar = 10 μm.

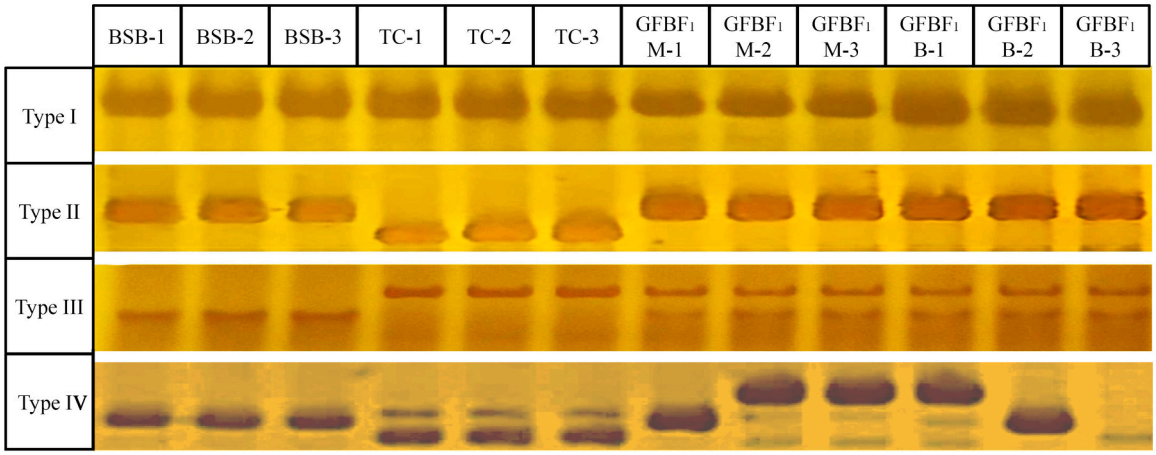

Fig. 4. Polyacrylamide electrophoresis diagrams of BSB, TC, $GBTF_1$-B, and $GBTF_1$-M. Type I: bands consistent with both BSB and TC in $GBTF_1$-B and $GBTF_1$-M. Type II: bands consistent with BSB but inconsistent with TC in $GBTF_1$-B and $GBTF_1$-M. Type III: bands consistent with TC but inconsistent with BSB in $GBTF_1$-B and $GBTF_1$-M. Type IV: bands inconsistent with both BSB and TC in $GBTF_1$-B and $GBTF_1$-M.

values of FL/BL, BL/BH, BL/HH, HL/HH of $GBTF_1$-B were also biased to BSB ($P > 0.05$). The number of lower lateral line scales and dorsal fin rays of $GBTF_1$-M was biased towards BSB ($P > 0.05$), but other countable and measurable traits of $GBTF_1$-M were between BSB and TC.

3.3. Determination of ploidy level

Following the successful preparation of $GBTF_1$, the DNA contents of $GBTF_1$-B, $GBTF_1$-M, BSB, and TC are shown in Fig. 2. The mean erythrocyte DNA content of BSB, TC, $GBTF_1$-B, and $GBTF_1$-M was 66.60, 68.81, 67.17, and 67.30, respectively. No significant difference was observed between $GBTF_1$ and the original parents ($P > 0.05$), which indicated that both $GBTF_1$-B and $GBTF_1$-M were diploid like BSB and TC. Moreover, the chromosome spreads of these four groups of fish are presented in Fig. 3. The chromosome spreads revealed that $GBTF_1$-B and $GBTF_1$-M had 48 chromosomes, consistent with their parental species.

3.4. Microsatellites analysis

The genetic composition of the two types of $GBTF_1$ was determined

Table 4
The statistics of micosatellite bands of $GBTF_1$-B and $GBTF_1$-M.

Category	Type I	Type II	Type III	Type IV	Total
$GBTF_1$-B1	68	65	27	16	176
$GBTF_1$-B2	71	57	24	15	167
$GBTF_1$-B3	66	67	22	16	171
Total number of $GBTF_1$-B	205	189	73	47	514
Percent of each type in $GBTF_1$-B	39.92 %	36.75 %	14.19 %	9.14 %	100 %
$GBTF_1$-M1	73	41	35	26	175
$GBTF_1$-M2	70	45	40	31	186
$GBTF_1$-M3	67	41	37	28	173
Total number of $GBTF_1$-M	210	127	112	85	534
Percent of each type in $GBTF_1$-M	39.36 %	23.77 %	20.97 %	15.90 %	100 %

by analyzing 20 pairs of microsatellite primers. A total of 1048 effective bands were obtained, including 514 bands from $GBTF_1$-B and 534 bands from $GBTF_1$-M. With BSB and TC as controls, microsatellite bands were classified into four types based on the polyacrylamide electrophoresis results (Fig. 4). Type I bands were consistent between BSB and TC, with both $GBTF_1$-B and $GBTF_1$-M exhibiting bands matching those of BSB and TC. Type II bands showed differences between BSB and TC, with the bands of both $GBTF_1$-B and $GBTF_1$-M being consistent with BSB. Type III bands also showed differences between BSB and TC, with both bands being present in $GBTF_1$-B and $GBTF_1$-M. Type IV bands of $GBTF_1$ were different from those of both BSB and TC; these bands may be attributed to mutation or recombination events. The statistics of the four types of microsatellite bands in $GBTF_1$-B and $GBTF_1$-M are shown in Table 4. In both $GBTF_1$-B and $GBTF_1$-M, the percentage of bands consistent with both BSB and TC was highest, at 39.92 % and 39.36 % respectively. In $GBTF_1$-B, the percentage of bands consistent with BSB or TC was 36.75 % and 14.19 %, respectively, and the percentage of bands inconsistent with BSB and TC which may be some "mutations" representing recombination events or other causes was 9.14 %. In $GBTF_1$-M, the percentage of bands consistent with BSB or TC was 23.77 % and 20.97 %, respectively, and the percentage of bands inconsistent with BSB and TC was 15.90 %.

3.5. Expression analysis of homologous genes

Second-generation transcriptome sequencing of RNA extracted from liver tissues of BSB, TC, $GBTF_1$-B, and $GBTF_1$-M yielded over 6 GB of raw data per sample. After mixing, assembling, and removing redundancies, a total of 102,795 transcripts were obtained, including 88,423,629 bp. The average length of transcripts was 860.19 bp, and the N50 was 1759 bp, with GC bases accounting for 44 %. Gene differential expression analysis revealed 42,516 homologous genes and 4615 DEGs. In $GBTF_1$-B (Fig. 5), 18.61–19.39 % of DEGs were up-regulated, 15.3–20.33 % of DEGs showed the ELD-BSB pattern, 6.96–8.43 % showed the ELD-TC pattern, 34.73–35.43 % of DEGs showed the additive pattern, and 17.81–24.40 % of DEGs were down-regulated. In $GBTF_1$-M (Fig. 5), DEGs were distributed as follows: 16.86–19.91 % exhibited up-

A

Type	Up regulation		ELD-BSB		ELD-TC		Additivity		Down regulation	
	I	II	III	IV	V	VI	VII	VIII	IX	X
	B H T	B H T	B H T	B H T	B H T	B H T	B H T	B H T	B H T	B H T
Diagram										
$GFBF_1$-B1	688	171	328	378	185	136	838	765	279	847
$GFBF_1$-B2	680	208	381	386	167	222	868	752	222	729
$GFBF_1$-B3	758	137	473	465	125	200	813	822	149	673
$GFBF_1$-M1	295	483	231	249	306	349	866	820	620	396
$GFBF_1$-M2	486	433	345	273	233	331	891	920	363	340
$GFBF_1$-M3	461	407	325	339	226	263	899	894	407	394
$GFBF_1$-B	18.61~19.39%		15.3~20.33%		6.96~8.43%		34.73~35.43%		17.81~24.40%	
$GFBF_1$-M	16.86~19.91%		10.40~14.39%		10.60~14.19%		36.53~39.24%		15.23~22.02%	

B

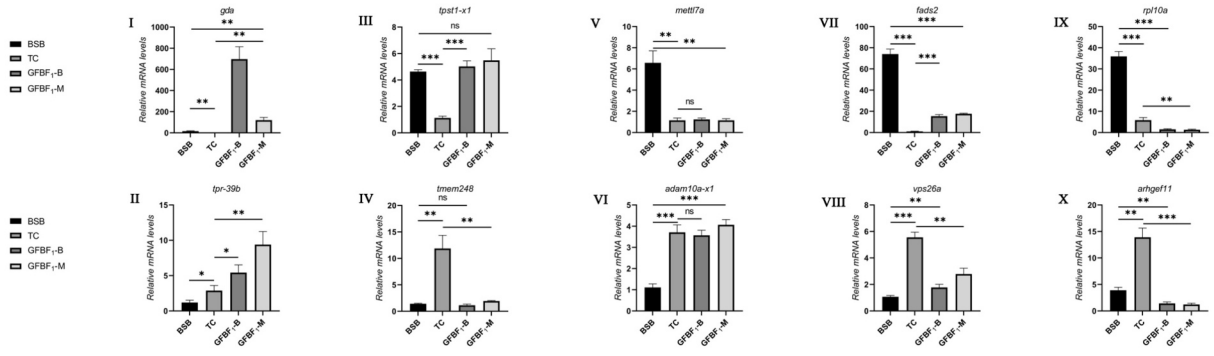

Fig. 5. The differences in expression modes of DEGs in $GBTF_1$-B and $GBTF_1$-M compared to BSB and TC. (A) Number and percentage of DEGs expressed in each expression mode in $GBTF_1$-B and $GBTF_1$-M. (B) qRT-PCR validation of expression modes of DEGs in BSB, TC, $GBTF_1$-B, and $GBTF_1$-M. Up-regulation: the expression level of DEGs in $GBTF_1$ was higher than in both BSB and TC. Down-regulation: the expression level of DEGs in $GBTF_1$ was lower than in both BSB and TC. ELD-BSB: the expression level of DEGs in $GBTF_1$ was practically equal to that in BSB. ELD-TC: the expression level of DEGs in $GBTF_1$ was practically equal to that in TC. Additive pattern: the expression level of DEGs in $GBTF_1$ was intermediate between in BSB and TC.

regulation, 10.40–14.39 % of DEGs showed the ELD-BSB pattern, 10.60–14.19 % exhibited the ELD-TC pattern, 36.53–39.24 % of DEGs showed the additive pattern, and 15.23–22.02 % were down-regulated.

In addition, in $GBTF_1$-B, the percentage of genes exhibiting the ELD-BSB pattern was higher than the percentage of genes showing the ELD-TC pattern ($P < 0.05$). However, in $GBTF_1$-M, the percentage of genes adopting the ELD-BSB pattern was only slightly lower than the percentage of genes showing the ELD-TC pattern. The results suggested that the gene expression of $GBTF_1$-B was more biased towards BSB while that of $GBTF_1$-M was intermediate. Ten representative genes from the above five expression modes were subjected to qRT-PCR to verify the presence of each expression mode in $GBTF_1$-B and $GBTF_1$-M, as displayed in Fig. 5 (B). The verification results were identical to the outcomes of the transcriptome analysis.

4. Discussion

Distant hybridization has been widely applied in genetic breeding of fish, with hybrid offspring exhibiting heterosis often used for aquaculture (Liu et al., 2025). The bisexually fertile progeny obtained can be used to produce a hybrid lineage (Liu, 2022). Artificial gynogenesis was also an important method for accelerating the selective breeding of varieties and populations (Li et al., 2023). However, many of the underlying genetic mechanisms remain unclear. In this research, gynogenetic progeny were obtained by inducing the eggs of the hybrid BTF_1 and doubling the chromosomes. Undoubled haploid eggs and triploid eggs with failed chromosome doubling or UV-treatmentfailed to develop. Flow cytometric analysis and chromosome preparation confirmed that both $GBTF_1$-B and $GBTF_1$-M are diploid with 48 chromosomes. According to the morphological traits, the progeny were classified into two types, namely $GBTF_1$-B and $GBTF_1$-M. These results indicate that BTF_1 produces only haploid gametes, which guarantees the establishment of distant hybridization and hybrid lineage between BSB and TC.

Microsatellites are widely used as molecular markers in analyzing the genetic inheritance and variation in eukaryotes due to their high polymorphism and high variability among species (Bao et al., 2016; Zane et al., 2002). $GBTF_1$-B developed a similar appearance to BSB, while $GBTF_1$-M displayed intermediate morphological characteristics between BSB and TC. However, the microsatellite analysis results determined that both $GBTF_1$-B and $GBTF_1$-M were genetic allodiploids containing heterologous genetic materials. Gene chimerism or recombination occurs in the hybrid offspring of many organisms (Lavinscky et al., 2017; Zhang et al., 2010; Zhao et al., 2020). Gene recombination at the genome level is common in the progeny of distant hybridization with heterologous genomes and has been validated in multiple studies (Huang et al., 2023; Liu et al., 2021). However, there was little research on whether these gene recombinations can be passed on through gametes. This finding discovered that gene recombination occurred between the two subgenomes from BSB and TC during the formation of BTF_1, and that this recombination can be transmitted to gametes via meiosis. Another possible explanation is recombination at the level of heterologous chromosomes, as the gametes of BTF_1 may contain chromosomes derived from both BSB and TC. However, this hypothesis requires further experimental validation.

Transcriptome analysis revealed that the gene expression of $GBTF_1$-B was biased towards BSB, suggesting that the proportion of genetic material of BSB may be significantly greater than that of TC in this type of fish. However, the expression level of $GBTF_1$-M was found to be intermediate between those of BSB and TC, with a slight bias towards TC. Therefore, the proportions of genetic material originating from BSB and TC may be comparable, and the proportion of TC may be greater than that of BSB. These results suggest that the heterologous genetic material originating from BSB and TC is unequally distributed in the gametes of BTF_1. This phenomenon may be attributed to heterologous chromosome pairing, complex meiotic behavior on exchange, and chromosomal structural variation such as gene chimerism and gene fusion.

No $GBTF_1$-T specimens were found in this study, the underlying reasons of which required further investigation to uncover. In addition, events such as crossing over or chromosomal translocation may occur during meiosis in the oocytes of BTF_1, leading to the presence of microsatellite bands containing both BSB and TC in the $GBTF_1$ individuals.

In this research, the eggs of BTF_1 were induced by using the inactivated sperm of common carp, yielding $GBTF_1$ after chromosome doubling. Microsatellite genotyping and transcriptomic expression analyses revealed that first-generation hybrid fish produce heterozygous gametes, which subsequently contribute to increased heterozygosity in the second-generation progeny. The research results provide an important basis for the establishment of hybrid lineages and for genome fusion analysis.

CRediT authorship contribution statement

Yingying Yang: Writing – original draft, Formal analysis, Conceptualization. **Lang Qin:** Methodology, Investigation. **Hongxuan Liang:** Validation, Software. **Jiawang Huang:** Methodology, Data curation. **Ming Wen:** Investigation. **Yuxiang Wang:** Supervision. **Le Shen:** Visualization. **Jinhui Huang:** Validation, Formal analysis. **Xu Huang:** Funding acquisition. **Fangzhou Hu:** Supervision, Conceptualization. **Shi Wang:** Supervision, Conceptualization. **Chang Wu:** Writing – review & editing, Project administration, Funding acquisition, Conceptualization. **Shaojun Liu:** Supervision, Project administration, Funding acquisition.

Declaration of competing interest

The authors declare the following financial interests/personal relationships which may be considered as potential competing interests:

Chang Wu AND Shaojun Liu reports financial support was provided by the National Natural Science Foundation of China (Grant Nos. 32102781, 32293250, 32293251). Chang Wu reports financial support was provided by Key Research and Development Program of Hunan Province (Grants No. 2023WK2001). Chang Wu reports financial support was provided by the Science and Technology Innovation Program of Hunan Province (Grants No. 2022RC1162). Xu Huang reports financial support was provided by Natural Science Foundation of Hunan Province, China (Grant No. 2024JJ6314). Xu Huang reports financial support was provided by Changsha Municipal Natural Science Foundation (Grant No. kq2402160). If there are other authors, they declare that they have no known competing financial interests or personal relationships that could have appeared to influence the work reported in this paper.

Acknowledgments

This research was financially supported by grants from the National Natural Science Foundation of China (Grant Nos. 32102781, 32293250, 32293251), Key Research and Development Program of Hunan Province (Grants No. 2023WK2001), The Science and Technology Innovation Program of Hunan Province (Grants No. 2022RC1162), Natural Science Foundation of Hunan Province, China (Grant No. 2024JJ6314), and Changsha Municipal Natural Science Foundation (Grant No. kq2402160).

Appendix A. Supplementary data

Supplementary data to this article can be found online at https://doi.org/10.1016/j.aquaculture.2025.743187.

Data availability

The complete clean reads for the libraries used in this study have been uploaded to the NCBI Sequence Read Archive (SRA) site (http://www.ncbi.nlm.nih. gov/sra/; BioProject ID: PRJNA1281314).

References

Anil, A., Gomelsky, B., Schneider, K.J., 2016. Variability in microsatellite DNA markers in gynogenetic and backcross progenies obtained from ornamental (koi) carp (C yprinus Carpio L.)× goldfish (C arassius auratus L.) hybrid females. Aquac. Res. 47, 1150–1155.

Ban, M., Nagoya, H., Sato, S., Yaegashi, H., Ichimura, M., Sato, N., 2013. Artificial and natural cross breeding between Atlantic salmon and salmonids currently present in Japan. Fish. Sci. 79, 967–975.

Bao, M.M., Zhou, Q., Xie, C.X., Cai, L.G., Niu, J.G., Li, H., 2016. Ten polymorphic microsatellite markers characterized for Schizothorax pseudaksaiensis and applied for population genetic analysis. J. Genet. 95, 5–8.

Brykov, V.A., Polyakova, N., Skurikhina, L., Dolganov, S., Eliseikina, M., Kovalev, M.Y., 2002. Mitochondrial DNA variation in goldfish Carassius auratus gibelio from far eastern water reservoirs. Russ. J. Genet. 38, 1176–1180.

Chen, R., Lou, B., Xu, D., Zhan, W., Takeuchi, Y., Yang, F., Liu, F., 2017. Induction of meiotic gynogenesis in yellow drum (Nibea albiflora, Sciaenidae) using heterologous sperm and evidence for female homogametic sex determination. Aquaculture 479, 667–674.

Chen, F., Li, X.-Y., Zhou, L., Yu, P., Wang, Z.-W., Li, Z., Zhang, X.-J., Wang, Y., Gui, J.-F., 2020. Stable genome incorporation of sperm-derived DNA fragments in gynogenetic clone of gibel carp. Mar. Biotechnol. 22, 54–66.

Fan, S., Tang, Z., Wang, Y., Zhou, Z., Wu, C., Luo, K., Hu, J., Gong, D., Li, S., Tao, M., 2024. The bisexual natural gynogenetic blunt snout bream lineage derived from the distant hybridization of female blunt snout bream and male Bleeker's yellow tail. Aquacult. Rep. 37, 102206.

Foster, J.T., Bull, R.L., Keim, P., 2020. Ricin forensics: comparisons to microbial forensics. In: Microbial Forensics. Elsevier, pp. 241–250.

Huang, X., Huang, J., Qin, L., Long, Y., Wu, C., Gong, K., Xiao, Q., Qin, Q., 2023. Full-length transcriptome reveals rapid genetic changes in triploid hybrid grass carp derived from female grass carp× male topmouth culter. Reprod. Breed. 3, 82–87.

Kukurba, K.R., Montgomery, S.B., 2015. RNA sequencing and analysis. Cold Spring Harb Protoc 2015 pdb. top084970.

Lavinscky, M., Souza, M., Silva, G., Melo, C., 2017. Contributions of classical and molecular cytogenetic in meiotic analysis and pollen viability for plant breeding. Genet. Mol. Res. 16, 1–15.

Li, T., Jia, Y., Gao, J., Zhao, J., Jiang, W., Gu, Z., Yang, R., 2018. Optimization of shock conditions to induce gynogenesis in topmouth culter (Culter alburnus). Aquaculture 490, 344–349.

Li, W., Zhou, Z., Tian, X., Li, H., Su, J., Liu, Q., Wu, P., Wang, S., Hu, J., Shen, Z., 2023. Gynogenetic Cirrhinus mrigala produced using irradiated sperm of Cyprinus carpio exhibit better cold tolerance. Reprod. Breed. 3, 8–16.

Liu, S., 2022. Fish Distant Hybridization. Springer.

Liu, S., Liu, Y., Zhou, G., Zhang, X., Luo, C., Feng, H., He, X., Zhu, G., Yang, H., 2001. The formation of tetraploid stocks of red crucian carp× common carp hybrids as an effect of interspecific hybridization. Aquaculture 192, 171–186.

Liu, Q., Luo, K., Zhang, X., Liu, F., Qin, Q., Tao, M., Wen, M., Tang, C., Liu, S., 2021. A new type of triploid fish derived from the diploid hybrid crucian carp (♀)× autotetraploid fish (♂). Reprod. Breed. 1, 122–127.

Liu, Q., Qi, Y., Liang, Q., Xu, X., Hu, F., Wang, J., Xiao, J., Wang, S., Li, W., Tao, M., 2018. The chimeric genes in the hybrid lineage of Carassius auratus cuvieri (♀)× Carassius auratus red var.(♂). Sci. China Life Sci. 61, 1079–1089.

Liu, S., Wang, S., Liu, Q., Wu, C., Zhou, Y., Tao, M., Zhang, C., Qin, Q., Luo, K., 2022. The research advances in animal distant hybridization and polyploid organisms. Fish Distant Hybrid. 1–37.

Liu, Q., Wang, S., Tang, C., Tao, M., Zhang, C., Zhou, Y., Qin, Q., Luo, K., Wu, C., Hu, F., 2025. The research advances in distant hybridization and gynogenesis in fish. Rev. Aquac. 17, e12972.

Luo, K., Xiao, J., Liu, S., Wang, J., He, W., Hu, J., Qin, Q., Zhang, C., Tao, M., Liu, Y., 2011. Massive Production of all-Female Diploids and Triploids in the Crucian Carp.

Mao, Z., Fu, Y., Wang, Y., Wang, S., Zhang, M., Gao, X., Luo, K., Qin, Q., Zhang, C., Tao, M., 2019. Evidence for paternal DNA transmission to gynogenetic grass carp. BMC Genet. 20, 1–7.

Marwal, A., Gaur, R.K., 2020. Molecular markers: tool for genetic analysis. In: Animal Biotechnology. Elsevier, pp. 353–372.

Miao, L., Tang, X.N., Li, M.Y., Wang, T., Wang, S., Zhang, X.L., Chen, J., 2014. Artificial gynogenesis in Pseudosciaena crocea (Perciformes, Sciaenidae) with heterologous sperm and its verification using microsatellite markers. Aquac. Res. 45.

Portemer, V., Renne, C., Guillebaux, A., Mercier, R., 2015. Large genetic screens for gynogenesis and androgenesis haploid inducers in Arabidopsis thaliana failed to identify mutants. Front. Plant Sci. 6, 147.

Qin, Q., Wang, J., Wang, Y., Liu, Y., Liu, S., 2015. Organization and variation analysis of 5S rDNA in gynogenetic offspring of Carassius auratus red var.(♀)× Megalobrama amblycephala (♂). BMC Genet. 16, 1–8.

Qin, Q., Huo, Y., Liu, Q., Wang, C., Zhou, Y., Liu, S., 2018. Induced gynogenesis in autotetraploids derived from Carassius auratus red var.(♀)× Megalobrama amblycephala (♂). Aquaculture 495, 710–714.

Rapp, R.A., Udall, J.A., Wendel, J.F., 2009. Genomic expression dominance in allopolyploids. BMC Biol. 7, 18.

Ren, L., Cui, J., Wang, J., Tan, H., Li, W., Tang, C., Qin, Q., Liu, S., 2017. Analyzing homoeolog expression provides insights into the rediploidization event in gynogenetic hybrids of Carassius auratus red var.× Cyprinus carpio. Sci. Rep. 7, 13679.

Sanguinetti, C.J., Simpson, A., 1994. Rapid silver staining and recovery of PCR products separated on polyacrylamide gels. Biotechniques 17, 914–921.

Su, X., Zheng, G., Jiang, X., Zou, S., 2019. Microsatellite markers analysis of two hybirds of Megalobrama terminalis× Erythroculter ilishaeformis, Megalobrama amblycephala× Erythroculter ilishaeformis. Acta Hydrobiol. Sin. 43, 264–271.

Sun, Y., Tao, M., Liu, S., Zhang, C., Duan, W., Shen, J., Wang, J., Zeng, C., Long, Y., Liu, Y., 2007. Induction of gynogenesis in red crucian carp using spermatozoa of blunt snout bream. Prog. Nat. Sci. 17, 163–167.

Tang, S., Bi, X., Wang, C., Zhang, F., Zhang, Y., Xie, Z., 2017. Genetic potential analysis of three selective breeding populations of blunt snout bream (Megalobrama amblycephala) using microsatellite markers. South China Fish. Sci. 13, 59–68.

Tóth, G., Gáspári, Z., Jurka, J., 2000. Microsatellites in different eukaryotic genomes: survey and analysis. Genome Res. 10, 967–981.

Wooten, J.A., Klooster, M.R., Brown, A.D., Bradford, P.R., Schwaner, T.D., Sullivan, B.K., 2018. Characterization of eight microsatellite markers for use in studies of genetic diversity and hybridization in Bufo microscaphus and Bufo woodhousii (Anura: Bufonidae) in Arizona, USA. J. Ariz. Nev. Acad. Sci. 47, 45–52.

Wu, Q., Ye, Y., Dong, X., 2003. Two unisexual artificial polyploid clones constructed by genome addition of common carp (Cyprinus carp) and crucian carp (Carassius auratus). Sci China C Life Sci 46, 595–604.

Wu, C., Chen, Q., Huang, X., Hu, F., Zhu, S., Luo, L., Gong, D., Gong, K., Zhao, R., Zhang, C., 2019. Genomic and epigenetic alterations in diploid gynogenetic hybrid fish. Aquaculture 512, 734383.

Wu, C., Huang, X., Chen, Q., Hu, F., Zhou, L., Gong, K., Fu, W., Gong, D., Zhao, R., Zhang, C., 2020. The formation of a new type of hybrid culter derived from a hybrid lineage of Megalobrama amblycephala (♀)× Culter alburnus (♂). Aquaculture 525, 735328.

Xiao, J., 2013. Establishment of Hybrid Strains between Blunt Snout Bream and Topmouth culter and their Genetic Characteristic Research. Hunan Normal University, Changsha.

Xiao, J., Zou, T., Chen, Y., Chen, L., Liu, S., Tao, M., Zhang, C., Zhao, R., Zhou, Y., Long, Y., 2011. Coexistence of diploid, triploid and tetraploid crucian carp (Carassius auratus) in natural waters. BMC Genet. 12, 1–15.

Xiao, J., Kang, X., Xie, L., Qin, Q., He, Z., Hu, F., Zhang, C., Zhao, R., Wang, J., Luo, K., 2014. The fertility of the hybrid lineage derived from female Megalobrama amblycephala× male Culter alburnus. Anim. Reprod. Sci. 151, 61–70.

Xu, K., Duan, W., Xiao, J., Tao, M., Zhang, C., Liu, Y., Liu, S., 2015. Development and application of biological technologies in fish genetic breeding. Sci. China Life Sci. 58, 187–201.

Yang, C., Dai, C., Liu, Q., Zhu, Y., Huang, X., Xu, X., Zhou, Y., Wang, S., Liu, Q., Liu, S., 2025. Different ploidy-level hybrids derived from female common carp× male topmouth culter. Aquaculture 594, 741366.

Zane, L., Bargelloni, L., Patarnello, T., 2002. Strategies for microsatellite isolation: a review. Mol. Ecol. 11, 1–16.

Zhang, S.G., Yang, W.H., Han, S.Y., Han, B.T., Li, M.X., Qi, L.W., 2010. Cytogenetic analysis of reciprocal hybrids and their parents between Larix leptolepis and Larix gmelinii: implications for identifying hybrids. Tree Genet. Genomes 6, 405–412.

Zhao, R., Wang, Y., Zou, L., Luo, Y., Tan, H., Yao, J., Zhang, M., Liu, S., 2020. Hox genes reveal variations in the genomic DNA of allotetraploid hybrids derived from Carassius auratus red var.(female)× Cyprinus carpio L.(male). BMC Genet. 21, 1–13.

Zhao, Y., Zhou, J., Dong, Y., Xu, D., Qi, D., 2024. Transcriptome analysis reveals the molecular mechanisms underlying growth superiority in a novel gymnocypris hybrid, gymnocypris przewalskii♀× gymnocypris ecklonii♂. Genes 15, 182.

Zheng, G., Wu, C., Liu, J., Chen, J., Zou, S., 2019. Transcriptome analysis provides new insights into the growth superiority of a novel backcross variety, Megalobrama amblycephala♀×(M. amblycephala♀× Culter alburnus♂)♂. Aquaculture 512, 734317.

Zhou, L., Wang, Y., Gui, J.-F., 2000. Genetic evidence for gonochoristic reproduction in gynogenetic silver crucian carp (Carassius auratus gibelio Bloch) as revealed by RAPD assays. J. Mol. Evol. 51, 498–506.

Zhou, Y., Ren, L., Xiao, J., Zhong, H., Wang, J., Hu, J., Yu, F., Tao, M., Zhang, C., Liu, Y., 2015. Global transcriptional and miRNA insights into bases of heterosis in hybridization of Cyprinidae. Sci. Rep. 5, 13847.

Zhou, H., Wang, Q., Zhou, Z.-Y., Li, X., Sun, Y.-Q., Shan, G., Zheng, X.-Y., Chen, Q., Liu, H.-J., Wang, W., 2022. Genome-wide DNA methylation and gene expression patterns of androgenetic haploid tiger pufferfish (Takifugu rubripes) provide insights into haploid syndrome. Sci. Rep. 12, 8252.